Article

Chinese Science Bulletin

Materials Science

August 2013 Vol.58 No.24: 3023–3032
doi: 10.1007/s11434-013-5863-6

Modeling of static coarsening of two-phase titanium alloy in the α+β two-phase region at different temperature by a cellular automata method

WU Chuan, YANG He* & LI HongWei

State Key Laboratory of Solidification Processing, School of Materials Science and Engineering, Northwestern Polytechnical University, Xi'an 710072, China

Received February 26, 2013; accepted April 10, 2013; published online May 20, 2013

A cellular automata (CA) method was employed to model static coarsening controlled by diffusion along grain boundaries at 1173 K and through the bulk at 1213 and 1243 K for a two-phase titanium alloy. In the CA model, the coarsening rate was inversely proportional to the 3rd power of the average grain radius for coarsening controlled by diffusion along grain boundaries, and inversely proportional to the 2nd power of the average grain radius for coarsening controlled by diffusion through the bulk. The CA model was used to predict the morphological evolution, average grain size, topological characteristics, and the coarsening kinetics of the Ti-6Al-2Zr-1Mo-1V (TA15) alloy during static coarsening. The predicted results were found to be in good agreement with the corresponding experimental results. In addition, the effects of the volume fraction of the α phase (V_f) and the initial grain size on the coarsening were discussed. It was found that the predicted coarsening kinetic constant increased with V_f and that a larger initial grain size led to slower coarsening.

CA model, morphology, coarsening kinetics, bulk diffusion-controlled, boundaries diffusion-controlled

Citation: Wu C, Yang H, Li H W. Modeling of static coarsening of two-phase titanium alloy in the α+β two-phase region at different temperature by a cellular automata method. Chin Sci Bull, 2013, 58: 3023–3032, doi: 10.1007/s11434-013-5863-6

Two-phase titanium alloys have been widely used in the aerospace industry because of their excellent moderate room-temperature and high-temperature strength [1–3]. For these types of alloys, static coarsening occurs easily during their application at higher temperatures, which usually has a large effect on the grain size, morphology, and phase volume fraction and, in turn, on the mechanical properties of the final parts. Therefore, investigation of the coarsening mechanism of such alloys at high temperatures is necessary for microstructure design and process control.

Over the years, many researchers have carried out experiments to study the static coarsening of two-phase titanium alloys in the β single phase field or the α+β two-phase field. It is generally believed that the static coarsening process can be expressed as a power law as a function of average grain size versus time [4],

$$d^n - d_0^n = K\left(t - t_0\right), \tag{1}$$

where d is the average grain diameter during coarsening, d_0 is the initial value at time t_0, K is the coarsening rate constant, and n is the coarsening exponent. Different values of n represent different coarsening mechanisms. Gil and Planell [4], Semiatin et al. [5], and Ivasishin et al. [6] investigated the static coarsening behavior of Ti-6Al-4V alloy in the β single phase field, and found that the value of n deviated from the theoretical value of 2 for pure metals under all temperatures tested. The authors attributed this difference to the effect of solute atoms, precipitates, or impurities [7]. However, for two-phase titanium alloys the coarsening mechanism in the α+β two-phase field is much more complicated than that in the β single phase field. Some authors, including Hu and Rath [8] and Grewal and Ankem [9,10],

*Corresponding author (email: yanghe@nwpu.edu.cn)

have systemically and experimentally studied the coarsening mechanisms of two-phase titanium alloys in the α+β two-phase field. All found that the value of n varied with temperature, and thus concluded that the controlling mechanism for the coarsening of two-phase titanium alloys in the α+β two-phase field may be mixed. Recently, Semiatin et al. [11] experimentally studied the static coarsening of Ti-6Al-4V alloy in the α+β two-phase field and also found that the value of n varied with temperature, with the coarsening mechanism being different at lower temperatures and higher temperatures.

However, some shortcomings are obvious when the coarsening process is studied experimentally. First, the experiments are time consuming. Second, direct observation of the coarsening process at high temperatures is unrealistic due to the limitations of the present experimental equipment [12]. In contrast, numerical modeling of static coarsening is an effective approach which not only enables visible reproduction of the virtual microstructural evolution, but also systematic and comprehensive investigation of the effects of volume fraction, morphology, and initial grain size on the coarsening process. The most used models for this purpose are the cellular automata method (CA) [13–15], the Monte Carlo method [16,17], and the phase field method [18–20]. Recently, many researchers have begun to simulate the grain coarsening of single phase alloys or multi-phase alloys in a single phase field. Geiger et al. [21] simulated the grain coarsening of a single phase alloy by a CA method based on the lowest-energy principle and discussed the effects of orientation differences, activation energy, and boundary energy on the coarsening. Subsequently, Raghavan and Sahay [22,23], and Kugler and Turk [24] simulated topological characteristics during the coarsening of polycrystalline materials in the single phase field. Recently, Wu et al. [25] studied the effects of solute drag on the coarsening kinetics of a near-α titanium alloy in the β single field by the CA method.

However, there is still a lack of information concerning the modeling of two-phase titanium alloys in the α+β two-phase field. The key reason for this is that the coarsening mechanism for two-phase titanium alloys in the α+β two-phase field is complicated. In the β single phase field, the coarsening process is driven by the reduction of interfacial free energy, which can easily be simulated by a CA method based on the lowest-energy principle. In contrast, the coarsening of two-phase titanium alloys in the α+β two-phase field is controlled by solute diffusion through the bulk (β-matrix), along grain boundaries (α–α or β–β grain boundaries), or across the interface (α–β phase interface). The volume fraction of the α or β phase varies with temperature due to phase transformation, which indicates that the coarsening mechanism may be different at different temperatures. Because it is difficult to accurately simulate the coarsening process of two-phase titanium alloys in the α+β two-phase field merely by the CA method using the lowest-energy principle, a new coarsening model is required.

In this study, the CA method was used to simulate the coarsening process of Ti-6Al-2Zr-1Mo-1V (TA15) alloy controlled by diffusion through the bulk at 1213 and 1243 K and along grain boundaries at 1173 K. To validate this CA model, the predicted grain size and size distribution were compared with corresponding experimental results. Furthermore, the effects of the volume fraction of the α phase and the initial average grain size on the coarsening process were discussed.

1 Coarsening mechanisms of two-phase titanium alloy in the α+β two-phase field

1.1 Coarsening controlled by diffusion through bulk

Based on the assumption of all grains having spherical structure, the change in the material quantity (in mole) of a larger grain over time dt can be given by

$$\frac{\mathrm{d}V}{V_{\mathrm{M}}\mathrm{d}t}=\frac{\mathrm{d}\left(\frac{4}{3}\pi r_1^3\right)}{V_{\mathrm{M}}dt}=\frac{4\pi r_1^2}{V_{\mathrm{M}}}\frac{\mathrm{d}r_1}{\mathrm{d}t}, \tag{2}$$

where dV is the volume change of the coarsening grain within time dt, r_1 is the radius of the larger grain, R is the gas constant, T is the absolute temperature, and V_{M} is the molar volume. Rate-controlling solute atoms are expelled into the matrix due to the shrinking of smaller grains. At the same time, the redundant solute atoms in the matrix gradually diffuse into the larger grain, which grows. The quantity of solute atoms diffusing into the larger grain within unit time can be given by

$$\chi 4\pi r_1^2\frac{C_2-C_1}{r_1}=\chi 4\pi r_1\cdot\frac{2\gamma V_{\mathrm{M}}C_1}{RT}\left(\frac{1}{r_2}-\frac{1}{r_1}\right), \tag{3}$$

with

$$C_2-C_1=\frac{2\gamma V_{\mathrm{M}}C_1}{RT}\left(\frac{1}{r_2}-\frac{1}{r_1}\right), \tag{4}$$

where χ is the diffusivity of the rate-limiting solute atoms in the matrix, r_2 is the radius of the smaller grain, C_1 is the equilibrium concentration of the rate-controlling solute atoms around the larger grain, C_2 is the equilibrium concentration of the rate-controlling solute atoms around the smaller grain, and γ is the interfacial energy. For a coarsening grain, the change in grain mass due to coarsening should be equal to that of the solute atoms diffusing into the grain. Thus, eq. (2) is equal to eq. (3), and

$$\frac{\mathrm{d}r_1}{\mathrm{d}t}=\frac{2\chi\gamma V_{\mathrm{M}}^2C_1}{RTr_1}\left(\frac{1}{r_2}-\frac{1}{r_1}\right). \tag{5}$$

In such a system there must be some grains that tend to grow, some that tend to shrink, and others that remain unchanged. In eq. (5), r_2 is assumed to be the average size and is rewritten as $\bar{r}$, while r_1 is any grain size, and thus eq. (5) can be rewritten as

$$\frac{\mathrm{d}r}{\mathrm{d}t}=\frac{2\chi\gamma V_{\mathrm{M}}^2 C_1}{RTr^2}\left(\frac{r}{\bar{r}}-1\right). \tag{6}$$

Obviously, when $r=2\bar{r}$, the value obtained for dr/dt is at a maximum $(\mathrm{d}r/\mathrm{d}t)_{\max}$. It is assumed that the value of $\mathrm{d}\bar{r}/\mathrm{d}t$ is approximately equal to $(\mathrm{d}r/\mathrm{d}t)_{\max}$ [26], thus,

$$\frac{\mathrm{d}\bar{r}}{\mathrm{d}t}=\frac{\chi\gamma V_{\mathrm{M}}^2 C}{2RT\bar{r}^2}. \tag{7}$$

The integral form of eq. (7) is given by

$$\bar{r}^3-\bar{r}_0^3=K_{\mathrm{bulk}}t, \tag{8}$$

with

$$K_{\mathrm{bulk}}=\frac{\chi\gamma V_{\mathrm{M}}^2 C_1}{2RT}, \tag{9}$$

where $\bar{r}_0$ and $\bar{r}$ represent the average grain size at time t_0 and t, respectively, and K_{bulk} is the coarsening rate constant.

1.2 Coarsening controlled by diffusion along grain boundaries

For coarsening controlled by diffusion along grain boundaries, it is assumed that the diffusion path has a rectangular cross-section. The width and height of the cross-section remains the same throughout the whole process, while the average length of the path increases with average grain size. The change in volume of the coarsening grain (in mole) over time dt is related to the cross-sectional area of the diffusion path, coarsening rate, and the concentration gradient of the rate-controlling solute atoms between the matrix and the coarsening grain, given by

$$\frac{\mathrm{d}\left(\frac{4}{3}\pi\bar{r}^3\right)}{V_{\mathrm{M}}\mathrm{d}t}=2\pi\bar{r}\xi\cdot M\frac{2\gamma}{\bar{r}}\cdot\left(\frac{C-C_1}{\bar{r}}\right), \tag{10}$$

where ξ is the width of the diffusion path, M is the mobility of the grain boundaries, C and C_1 are the concentration gradient of the rate-controlling solute atoms in the matrix and the coarsening grain, respectively. Eq. (10) can be rewritten as

$$\frac{\mathrm{d}\bar{r}}{\mathrm{d}t}=\frac{K_{\mathrm{boun}}}{\bar{r}^3}, \tag{11}$$

where K_{boun} is the coarsening rate constant for boundary diffusion-controlled coarsening. The integral form of eq. (11) can be written as

$$\bar{r}^4-\bar{r}_0^4=K_{\mathrm{boun}}t, \tag{12}$$

with

$$K_{\mathrm{boun}}=V_{\mathrm{M}}\xi M\gamma\left(C-C_1\right). \tag{13}$$

2 CA models for coarsening of two-phase titanium alloy in the α+β two-phase field

In a CA model, each cell is characterized in terms of boundary conditions, neighborhood, state variables, and transition rules [14]. In this study, the cell was selected to be a regular square with a periodic boundary condition and an 8-cell neighborhood. Several state variables including phase state, orientation, coarsening rate, and coarsening distance were assigned to each cell. The transition rules were defined as a function of the previous state of a lattice point in each cell and the state of the neighboring sites.

For the CA modeling of grain coarsening, the energy of each cell comprises two parts: thermal energy (E_{t}) and boundary energy (E_{b}). The value of E_{t} is determined by assigning a random number to every cell at each simulation step using a computer program [13],

$$E_{\mathrm{t}}=-RT\ln r\_num, \tag{14}$$

where *r_num* (0<*r_num*<1) is a random number produced by the computer program. In this model, each cell is assigned a real number q (0<q⩽180.0) to represent its orientation. The misorientation angle θ between two neighboring grains is determined as a function of the difference in orientation between the two grains, which is given by

$$\theta=\frac{\pi}{2}\times\left|\frac{\Delta q}{q_{\max}}\right|, \tag{15}$$

where Δq is the orientation difference between two adjacent grains and $q_{\max}$ is the maximum orientation number. The boundary energy is a function of θ between the two neighboring grains, and its value on the ith side of a cell is given by [21],

$$E_{\mathrm{b}}^i=E_0\sin(\theta)\left[1-\ln\left(\sin(\theta)\right)\right]\left(1-\delta_{q_iq_j}\right), \tag{16}$$

with

$$E_{\mathrm{b}}=\sum E_{\mathrm{b}}^i, \tag{17}$$

where E_0 is the energy of the high-angle grain boundary, q_i and q_j are the randomly assigned orientation values, and δ is the Kronecher symbol.

During a real coarsening process, coarsening is realized by the jumping of atoms on the grain boundaries from one side to another. Only atoms with enough energy to overcome the self-diffusion activation energy Q_{act} may migrate. However, in a CA coarsening model this process comprises two steps.

The first step is to compare the total energy of a cell on

the boundary with Q_{act}. This step is carried out to determine whether the cell may be selected as a potential transition cell. If its total energy is greater than Q_{act}, the cell can be selected as a transition cell with a selected probability, P_s, of one. Otherwise, the cell is selected as a transition cell with P_s, which is given as follows [27]:

$$P_s = \exp\left(\frac{-\Delta E}{RT}\right), \tag{18}$$

where ΔE is the difference in the total energy of a cell before and after its transition. Therefore, the selected probability of a cell can be given as follows:

$$P_s = \begin{cases} 1 & E_t + E_b > Q_{act} \\ \exp\left(\dfrac{-\Delta E}{RT}\right) & E_t + E_b < Q_{act}. \end{cases} \tag{19}$$

The second step is to determine the transition probability P_t of a selected cell. The migration distance of the grain boundary where a cell (i, j) is located over time t is determined by

$$l_{i,j}^t = \int_0^t v\Delta t\,, \tag{20}$$

where v is the coarsening rate (or migration rate of the grain boundary) determined by eqs. (7) or (11). In the CA model, whether a cell state may be changed or not is determined by the ratio of migration distance to side length of the cell, given in ref. [28] as

$$f_{i,j}^t = l_{i,j}^t / L\,, \tag{21}$$

where L is the side length of a cell. If the ratio is no less than 1.0, the cell state variables convert into new values and the value of l is reset to zero.

The state variables of the cells are updated by the synchronous application of the transition rules acting on them. Details of the CA transition rules for the current simulation are outlined below. (1) The values of the thermal and boundary energy of each cell on the grain boundaries are calculated according to eqs. (14) and (17). The total energy of each cell is then compared with the self-diffusion activated energy. If the difference between them is larger than 0, the value of P_s is set as 1 and the cell becomes a cell with the potential to change its state variables; otherwise, P_s is determined by eq. (18). At the same time, a random number r_num ($0<r\_num<1$) is generated by the computer code, and if the value of P_s is no less than the random number, the cell becomes a selected one. (2) For coarsening controlled by diffusion through bulk, the coarsening rate depends on the 2nd power of the average grain radius (according to eq. (7)), while the coarsening rate depends on the 3rd power of average grain radius (according to eq. (11)) for the coarsening controlled by diffusion along grain boundaries. (3) The values of $l_{i,j}^t$ and $f_{i,j}^t$ can then be determined according to eqs. (20) and (21). The value of $f_{i,j}^t$ determines whether the cell state variables can be updated or not. If the value is no less than 1, the state variables of the cell change into those of one of its neighboring cells and grain coarsening occurs. At the same time, the growth length loses its meaning and is set to zero again. Otherwise, the growth distance continues evolving according to eq. (20). (4) After the above mentioned steps, the state variables of each cell on the boundaries and their neighboring cells are updated, and the microstructural evolution of the CA model proceeds. The above transition rules can be illustrated as shown in Figure 1.

3 Experimental

The material used in the present work was a type of near α-titanium alloy, TA15, which had a measured chemical composition (in wt.%) of 6.06 aluminum (Al), 2.08 molybdenum (Mo), 1.32 vanadium (V), 1.86 zirconium (Zr), balance titanium, as shown in Table 1. The β-transus temperature (temperature at which $\alpha+\beta\rightarrow\beta$) of the alloy was determined to be 1263 K. The microstructure of the as-received material consisted of a bimodal α+β structure of approximately 60% primary α within the transformed β

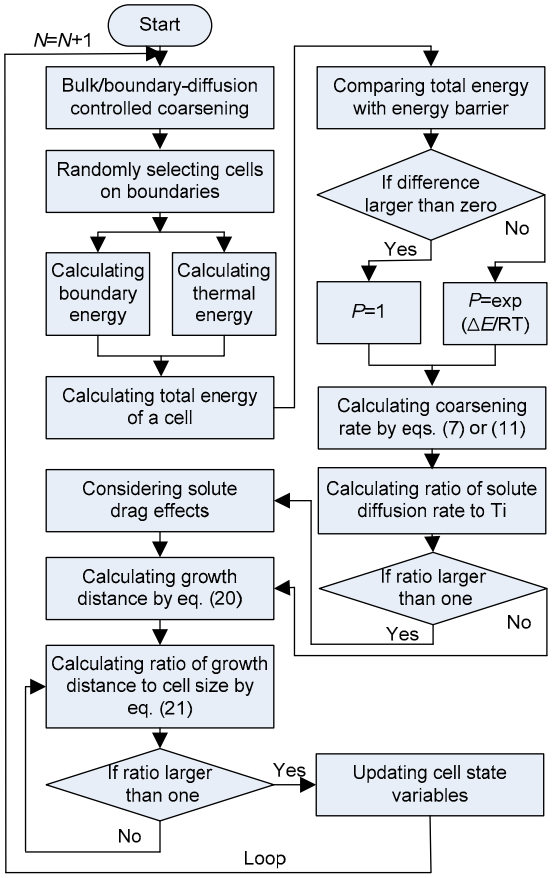

Figure 1 Flow chart of CA transition rules.

matrix. The material was soaked at temperatures of 1173, 1213, and 1243 K for 0.5 to 60 h, as shown in Table 2, to obtain different coarsened grain sizes. After the heat treatment procedures, standard metallographical techniques were used to determine the average grain size of the primary α phase. Considering the non-spherical shapes of the α grains, the radius r_i of the ith α grain was approximately calculated by $r_i = \sqrt{A_i/\pi}$, where A_i is the equivalent area of the ith grain. The average grain radius at each time step was then calculated as $\overline{r} = \frac{1}{N}\sum_i^N r_i$, where N is the total number of grains.

Table 1 The chemical composition of TA15 alloy

Solute elements	Ti	Al	Mo	Zr	V	Fe	Others
Fraction (wt.%)	Balance	6.06	2.08	1.86	1.32	0.3	<0.25

Table 2 Heat treatment experiments

Temperature (K)	Soaking time (h)							
1173	0.5	1	2.5	5	12	24	48	60
1213	0.5	1	2.5	5	12	24	48	60
1243	0.5	1	2.5	5	12	24	48	60

4 Simulation results

4.1 Morphology evolution

Figure 2 shows the typical microstructure simulated by the CA method for treatment temperatures of 1173, 1213, and 1243 K, respectively, and reveals remarkable changes in the morphology and size of the α grains. It is evident that the temperature and soaking time have significant influences on the microstructural evolution. Overall, the morphology of the α grains evolves toward equiaxed or spherical structure with time at a given temperature. The average grain size increases with time at a specific temperature. The longer the soaking time, the larger the average grain size becomes during coarsening. As expected, the larger grains (more than six sides) grow and the smaller grains (less than six sides) shrink during the coarsening process, with the volume fraction of the α phase remaining approximately constant. Figure 3(a) shows the evolution of microstructural uniformity

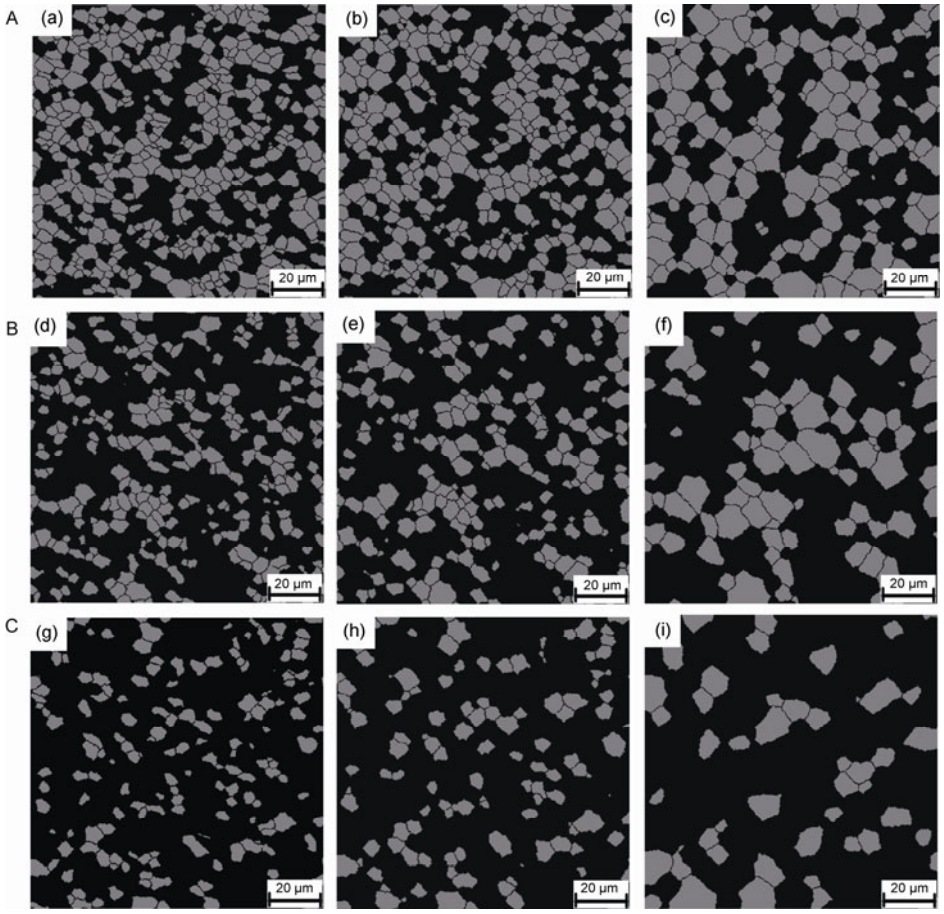

Figure 2 The microstructure simulated via the CA method at (A) 1173, (B) 1213, and (C) 1243 K with different time. (a), (d), (g) 0.5 h; (b), (e), (h) 5 h; (c), (f), (i) 48 h.

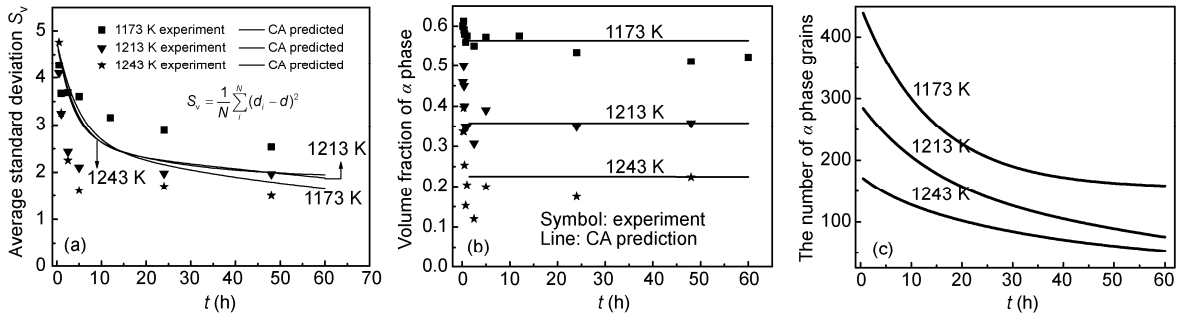

Figure 3 The evolution of (a) microstructural uniformity, (b) volume fraction of α phase, and (c) the number of α phase grains with time.

(S_v) with time, where $S_v = \frac{1}{N}\sum_i^N (d_i - d)^2$. It can be seen that the predicted values of S_v (fitting curves in Figure 3(a)) become smaller with time under the test temperatures, which better matches the experimental measurements (scatter points). Figure 3(b) shows a comparison of the predicted α phase volume fractions with the experimental values. It can be seen that the volume fraction remains nearly constant throughout the process and calculated and experimental values show good agreement after 1 h. The evolution of the number of α phase grains with time is shown in Figure 3(c). At 1173 K, the number of α phase grains is higher than those obtained at other temperatures. The number gradually decreases with increasing temperature.

4.2 Topology characteristics

Topological evolution is an important index characterizing the coarsening behavior. The side distribution of the α grains predicted by the CA method is shown in Figure 4, obtained by plotting the frequency of occurrence of grains with different numbers of sides. Similar to the experimental observations, the predicted maximum frequency of the distribution belongs to grains with 6 sides, which had a volume fraction of up to 30%, followed by grains with 5 or 7 sides, with a volume fraction of up to 40%. Nearly 20% of the grains had 4 or 8 sides. The volume fraction of grains with less than 3 or more than 10 sides is no more than 5%. These figures (Figure 4(a)–(c)) also indicate that the side distribution is close to normal distribution. The shapes of the distribution curves match better with the experimental results.

The grain size distribution (GSD) is another important index characterizing the coarsening behavior. To further validate the CA models, the GSD predicted by the CA modeling was compared with the experimental values. Figure 5 shows the normalized GSD results obtained from the CA simulations (histograms with dot-dashed lines) and the experiments (histograms with solid lines). It can be seen that the predicted results agree well with the experimental measurements. At 1173 K, the maxima of the GSD from the CA modeling and the experiments are close to a $u=d_i/d$ value of 1. However, the shapes of the GSD more or less deviate from self-similarity. Furthermore, the number of α phase grains with having size greater than the average value varies with time. This results in a broader GSD with a longer tail. These characteristics are obviously different from those reported by Semiatin et al. [11], and may be caused by a different coarsening mechanism. At 1173 K in the present study, the coarsening process is controlled by diffusion along boundaries instead of through the bulk. In addition, grain coalescences in the experiments or CA simulation could change the shape of the GSD [29,30]. However, at 1213 and 1243 K, the coarsening mechanisms are controlled by diffusion through the bulk, and thus the GSD shapes remain nearly time-invariant and are close to those in Semiatin et al.'s work [11].

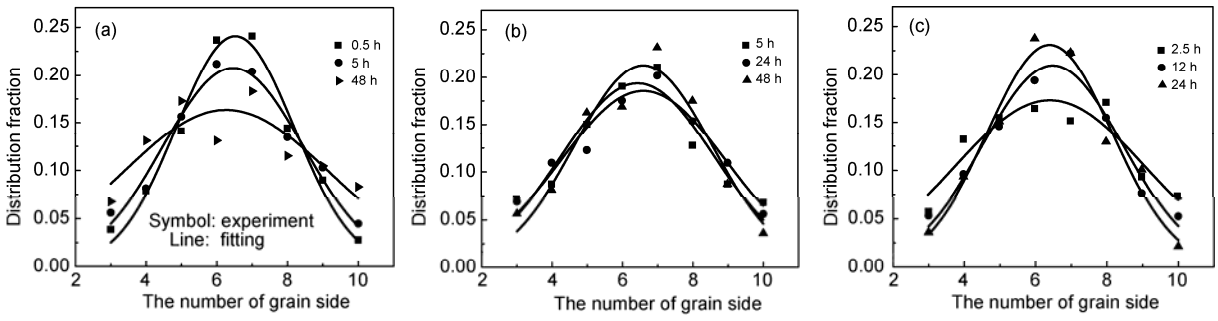

Figure 4 The grain side distribution at different temperatures. (a) 1173 K, (b) 1213 K, (c) 1243 K.

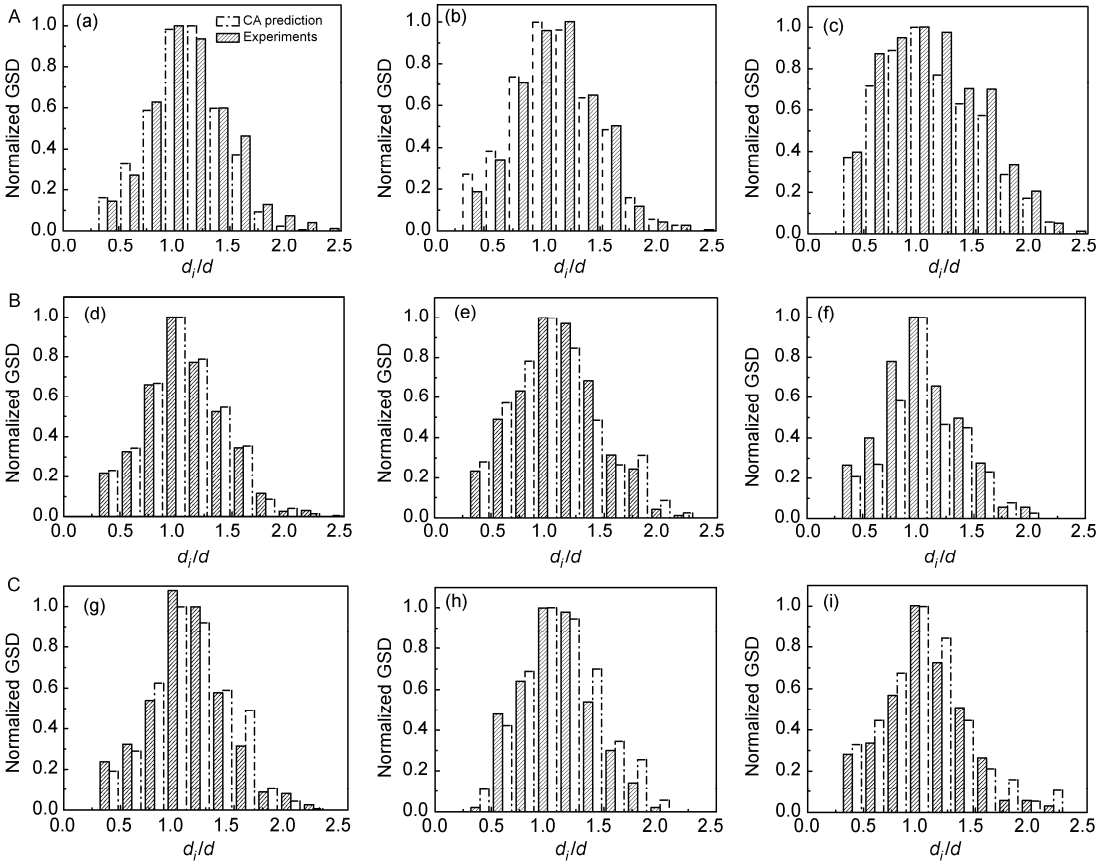

Figure 5 The comparisons of the predicted GSD with the experimental at 1173 (A), 1213 (B) and 1243 K (C) with different time. (a), (d), (g) 0.5 h; (b), (e), (h) 5 h; (c), (f), (i) 48 h.

4.3 Coarsening rate constant *K*

Figure 6 shows the kinetic curves obtained from the CA simulation (curves in black) and the experimental values (black scatter points) at 1173, 1213, and 1243 K. As shown in the figures, the predicted average grain size agrees well with the experimental data. The predicted grain size increases with temperature or time, as observed in the experiments. The time has an important effect on the coarsening rate (slope of the curve). The coarsening rate increases rapidly during the initial stages, but gradually drops with time. This may be caused by the decrease in grain boundary area (energy) per unit volume with time. Therefore, the driving force for the coarsening is lowered and the coarsening process becomes slow.

According to eq. (1), the value of K at different temperature can be obtained from the slope of a plot of $d^n - d_0^n$ vs. $t - t_0$, as shown in Figure 7. It is observed that the slope of the fitting line (or the value of K) increases with decreasing temperature. At 1173 K, the value of K (or the slope) is 458, significantly greater than the values of 53.3 and 32.5 obtained at 1213 and 1243 K, respectively. The difference between them may be caused by the following reasons. First, the coarsening mechanisms are different under these different temperatures. At the lower temperature of 1173 K, coarsening is controlled by the diffusion of solute atoms along boundaries. For this type of coarsening, the solute atoms diffuse along α–α or β–β grain boundaries, which are defect areas with high stored energy. This may provide more energy for the atoms to overcome the energy barriers. Thus, the diffusion process takes place easily and the value of K is larger. At 1213 and 1243 K, however, coarsening is controlled by diffusion through bulk and thus the diffusing atoms have to overcome lattice, dislocation, and other impurity atoms. Therefore, the coarsening process is inhibited to some extent and the value of K is relatively smaller than that at 1173 K. Second, the effect of the volume fraction of the α phase (V_f) on K is evident, and has been reported in many studies [31,32]. At low temperature, V_f is higher, so more grain boundaries are able to serve as diffusion paths for solute atoms. In addition, the elastic interaction between the different grains becomes more significant, which leads to a higher elastic energy stored near the boundary areas. Thus, the value of K may increase with increasing V_f or decreasing temperature. However, the value of K at 1213 K is slightly larger than that at 1243 K, despite the coarsening mechanism remaining the same. This may be caused by the fact that the diffusion distance between different α grains at

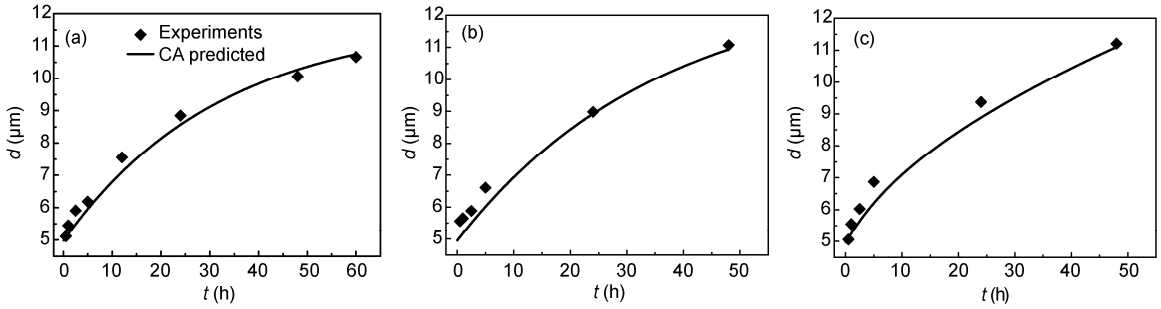

Figure 6 The comparisons of the predicted coarsening kinetics with the experimental at (a) 1173 K, (b) 1213 K, and (c) 1243 K.

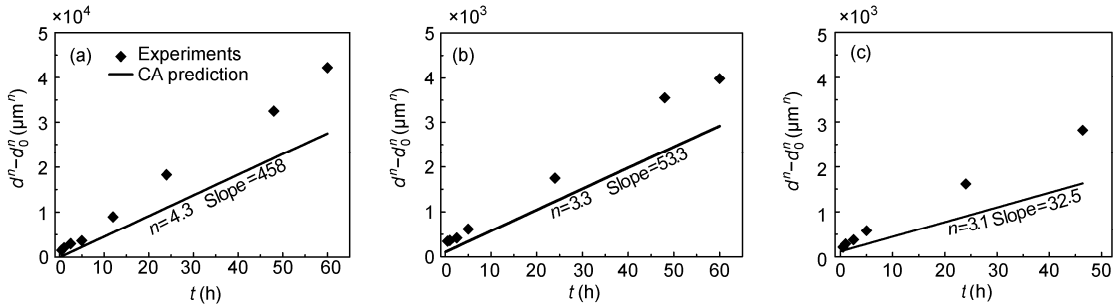

Figure 7 The coarsening rate constant predicted by the CA method (black lines) at temperature (a) 1173 K, (b) 1213 K, and (c) 1243 K.

1213 K is relatively smaller than that at 1243 K. Therefore, a more rapid coarsening process takes place and the value of K is slightly larger at 1213 K than that at 1243 K.

5 Discussion

5.1 Effect of volume fraction of α phase

The coarsening kinetics of the alloy with different values of V_f at 1173, 1213, and 1243 K are predicted as shown in Figure 8(a)–(c), respectively. It is evident that V_f has an important effect on the coarsening kinetics, and an increase in V_f (or a decrease in volume fraction of the β phase) at a given temperature accelerates the coarsening process. The values of K are also sensitive to V_f. At 1173 K, for example, the value of K is in the range of 51.8 to 570 with V_f increasing from 31.2% to 69.7%, as shown in Figure 8(a). Similarly, the value of K increases with V_f at 1213 and 1243 K. Grewal and Ankem [9,10] also reported this phenomenon in their studies of the coarsening behavior of α–β titanium alloys. This phenomenon may be explained as follows. In the present study, at 1173 K, the coarsening of the α phase is controlled by diffusion along grain boundaries. If the value of V_f increases, more grain boundaries serve as diffusion paths. Furthermore, the elastic interactions between the different grains become more evident with increasing V_f, leading to a higher elastic energy stored near the boundary area. Both of the above reasons may accelerate the coarsening process and thus result in a higher coarsening rate constant. At 1213 and 1243 K, the coarsening process is controlled by solute diffusion through the bulk. It is clear that the diffusion distance enlarges with decreasing V_f, and thus a much longer time is required to complete the solute diffusion, which results in a slower coarsening process.

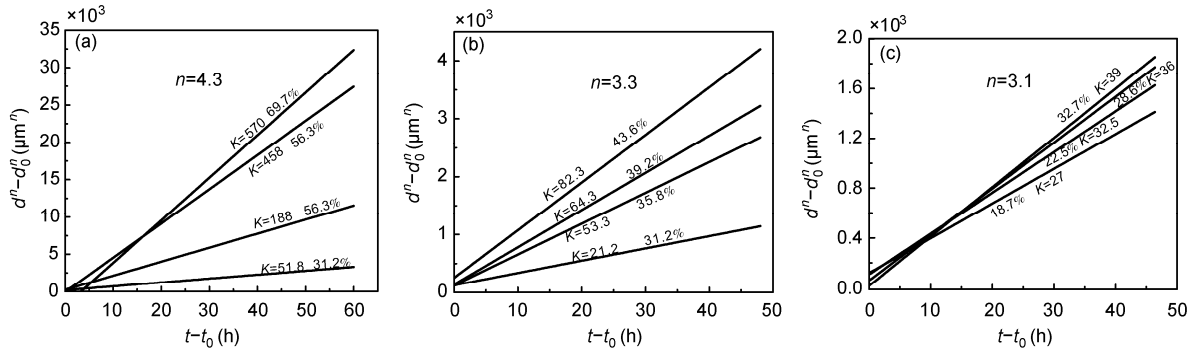

Figure 8 The effect of volume fraction of α phase on coarsening kinetics predicted by CA method at temperatures (a) 1173 K, (b) 1213 K, (c) 1243 K.

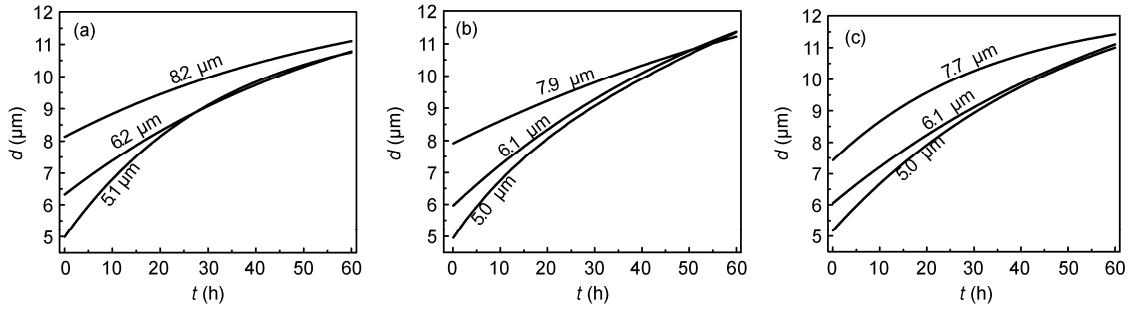

Figure 9 The effect of initial grain size on coarsening kinetics predicted by CA method at temperature (a) 1173 K, (b) 1213 K, and (c) 1243 K.

5.2 Effect of initial grain size

Figure 9 shows the effects of initial grain size (d_0) on coarsening behavior, where the number on each curve represents the initial grain size. It can be seen that the effects are significant. The coarsening rate (curvature) becomes smaller with increasing initial grain size for all the test temperatures, e.g. the larger the initial grain size, the smaller the coarsening rate becomes. For any given value of d_0, the coarsening process is faster during the initial stages, while it gradually slows with time and eventually stops. It can also be seen from these figures that the average grain size d increases with d_0. The difference in average grain size between the different d_0 becomes smaller with time. For example, as shown in Figure 9(a), the average grain size with d_0 of 5.1 μm gradually becomes close to that with d_0 of 8.2 μm with time. A similar characteristic is observed at a temperature of 1213 or 1243 K, as shown in Figure 9(b) and (c). For coarsening controlled by diffusion through the bulk or along grain boundaries, the solute atom diffusion distance is directly related to the initial grain size. In a system with a fixed value of V_f, a smaller value of d_0 usually leads to a larger α–α grain boundary area, which provides more diffusion paths for solute atoms and thus a faster coarsening rate is produced. Similarly, a smaller d_0 may also result in a shorter diffusion distance between the different grains, which may also accelerate the coarsening process. The average grain size increases with time and the effect of d_0 becomes minor.

6 Conclusions

A CA method was employed to simulate static coarsening of the TA15 alloy in the α+β two-phase field, namely, coarsening controlled by diffusion along grain boundaries at 1173 K and coarsening controlled by diffusion through the bulk at 1213 and 1243 K. The effects of the volume fraction of the α phase and the initial grain size on the coarsening were discussed. Some conclusions were obtained as follows: (1) The predicted average grain size and the size distribution during coarsening were compared with the experimental results, which was found to be in good agreement with the corresponding experimental results. This validates the CA model. (2) The simulated results showed that the grain morphology gradually evolved toward equiaxed or spherical structure with time at 1173, 1213 and 1243 K; the average grain size increased with time at a specific temperature. (3) The coarsening rate and coarsening rate constant increased with the increasing volume fraction of the α phase; the coarsening rate decreased with the increasing initial grain size under the test temperatures

This work was supported by the National Natural Science Foundation of China (50935007, 51175428), the National Basic Research Program of China (2010CB731701), the Foundation for Fundamental Research of Northwestern Polytechnical University in China (NPU-FFR-JC20100229), and the Center for Foreign Talent Introduction and Academic Exchange for Advanced Materials and Forming Technology Discipline Project (B08040).

1 Huang L J, Geng L, Li A B, et al. Characteristics of hot compression behavior of Ti-6.5Al-3.5Mo-1.5Zr-0.3Si alloy with an equiaxed microstructure. Mater Sci Eng A, 2009, 505 :136–143
2 Vo P, Jahazi M, Yue S. Recrystallization during thermomechanical processing of IMI834. Metall Trans A, 2008, 39: 2956–2980
3 Vo P, Jahazi M, Yue S, et al. Flow stress prediction during hot working of near-alpha titanium alloys. Mater Sci Eng A, 2007, 447: 99–110
4 Gil F J, Planell J A. Behaviour of normal grain growth kinetics in single phase titanium and titanium alloys. Mater Sci Eng A, 2000, 283: 17–24
5 Semiatin S L, Fagin P N, Glavicic M G, et al. Influence on texture on beta grain growth during continuous annealing of Ti-6Al-4V. Mater Sci Eng A, 2001, 299: 225–234
6 Ivasishin O M, Semiatin S L, Markovsky P E, et al. Grain growth and texture evolution in Ti-6Al-4V during beta annealing under continuous heating conditions. Mater Sci Eng A, 2002, 337: 88–96
7 Wang T, Guo H Z, Tan L J, et al. Beta grain growth behavior of TG6 and Ti17 titanium alloys. Mater Sci Eng A, 2011, 528: 6375–6380
8 Hu H, Rath B B. On the time exponent in isothermal grain growth. Metall Trans, 1970, 1: 3181–3184
9 Grewal G, Ankem S. Isothermal particle growth in two-phase titanium alloys. Metall Trans A, 1989, 20: 39–54
10 Grewal G, Ankem S. Particle coarsening behavior of alpha and beta titanium alloys. Metall Trans A, 1990, 21: 1645–1654
11 Semiatin S L, Kirby B C, Salishchev G A. Coarsening behavior of an alpha-beta titanium alloy. Metall Mater Trans A, 2004, 35: 2809–2819
12 Sharma H, Huizenga R M, Bytchkov A, et al. Observation of chang-

ing crystal orientations during grain coarsening. Acta Mater, 2012, 60: 229–237
13 He Y Z, Ding H L, Liu L F, et al. Computer simulation of 2D grain growth using a cellular automata model based on the lowest energy principle. Mater Sci Eng A, 2006, 429: 236–246
14 Raabe D, Becker R C. Coupling of a crystal plasticity finite-element model with a probabilistic cellular automaton for simulating primary static recrystallization in aluminum. Model Simul Mater Sci Eng, 2000, 8: 445–462
15 Rollett A D, Raabe D. A hybrid model for mesoscopic simulation of recrystallization. Comput Mater Sci, 2001, 21: 69–78
16 Song X Y, Liu G Q, Gu N J. A new Monte Carlo simulation of three-dimensional microstructures and their evolution in polycrystalline. Chin Sci Bull, 1999, 44: 1432–1436
17 Tong M M, Li D Z, Li Y Y. Modeling the austenite-ferrite diffusive transformation during continuous cooling on a mesoscale using Monte Carlo method. Acta Mater, 2004, 52: 155–1162
18 Kim D M, Ardell A J. Coarsening of Ni_3Ge in binary Ni-Ge alloys: Microstructures and volume fraction dependence of kinetics. Acta Mater, 2003, 51: 4073–4082
19 Boisse J, Lecoq N, Patte R, et al. Phase-field simulation of coarsening of γ precipitates in an ordered γ' matrix. Acta Mater, 2007, 55: 6151–6158
20 Luo B C, Wang H P, Wei B B. Phase field simulation of monotectic transformation for liquid Ni-Cu-Pb alloys. Chin Sci Bull, 2009, 54: 183–188
21 Geiger J, Roósz A, Barkóczy P. Simulation of grain coarsening in two dimensions by cellular automaton. Acta Mater, 2001, 49: 623–629
22 Raghavan S, Sahay S S. Modeling the grain growth kinetics by cellular automaton. Mater Sci Eng A, 2007, 445–446: 203–209
23 Raghavan S, Sahay S S. Modeling the topological features during grain growth by cellular automaton. Comput Mater Sci, 2009, 46: 92–99
24 Kugler G, Turk R. Study of the influence of initial microstructure topology on the kinetics of static recrystallization using a cellular automata model. Comput Mater Sci, 2006, 37: 284–291
25 Wu C, Yang H, Li H W, et al. Static coarsening for titanium alloys in single field by cellular automata considering solute atoms drag and anisotropic mobility. Chin Sci Bull, 2012, 57: 1473–1482
26 Greenwood G W. The growth of dispersed precipitates in solutions. Acta Metall, 1956, 4: 243–248
27 Chen F, Cui Z S, Liu J. Mesoscale simulation of the high-temperature austenitizing and dynamic recrystallization by coupling a cellular automaton with a topology deformation technique. Mater Sci Eng A, 2010, 527: 5539–5549
28 Zheng C W, Xiao N M, Li D Z, et al. Microstructure prediction of the austenite recrystallization during multi-pass steel strip hot rolling: A cellular automaton modeling. Comput Mater Sci, 2008, 44: 507–514
29 Zhu J Z, Wang T, Ardell A J, et al. Three-dimensional phase-field simulations of coarsening kinetics of c_0 particles in binary Ni-Al alloys. Acta Mater, 2004, 52: 2837–2845
30 Vaithyanathan V, Chen L Q. Coarsening of ordered intermetallic precipitates with coherency stress. Acta Mater, 2002, 51: 4061–4073
31 Ma Y, Ardell A J. Coarsening of γ (Ni-Al solid solution) precipitates in a γ' matrix: A striking contrast in behavior from normal γ/γ' alloys. Scripta Mater, 2005, 52: 1335–1340
32 Wang T, Guang S, Liu Z K, et al. Coarsening kinetics of γ' precipitates in the Ni-Al-Mo system. Acta Mater, 2008, 56: 5544–5551